International Journal of Bifurcation and Chaos, Vol. 1, No. 2 (1991) 417–430

54

COMPUTATIONAL UNFOLDING OF DOUBLE-CUSP MODELS OF OPINION FORMATION

RALPH ABRAHAM, ALEXANDER KEITH, and MATTHEW KOEBBE
Mathematics Department, University of California, Santa Cruz, CA 95064, USA

GOTTFRIED MAYER-KRESS
Mathematics Department, University of California, Santa Cruz, CA 95064, USA and Center for Nonlinear Studies, Los Alamos National Laboratories, Los Alamos, NM 87545, USA

In 1975, Isnard and Zeeman proposed a cusp catastrophe model for the polarization of a social group, such as the population of a democratic nation. Ten years later, Kadyrov combined two of these cusps into a model for the opinion dynamics of two "nonsocialist" nations. This is a nongradient dynamical system, more general than the double-cusp catastrophe studied by Callahan and Sashin [1987]. Here, we present a computational study of the nongradient double cusp, in which the degeneracy of Kadyrov's model is unfolded in codimension eight. Also, we develop a discrete-time cusp model, study the corresponding double cusp, establish its equivalence to the continuous-time double cusp, and discuss some potential applications. We find bifurcations for multiple critical-point attractors, periodic attractors, and (for the discrete case) bifurcations to quasiperiodic and chaotic attractors.

1. Introduction

We study a family of models motivated by applications in the social sciences.

Background

Isnard and Zeeman have introduced a style of application of catastrophe theory for the social sciences. In an exemplary model, the cusp catastrophe is applied explicitly to a country whose leadership is responsive to the opinions of its people. It models the split of the people into two groups, hawks and doves, on the basis of their foreign-policy positions [Isnard & Zeeman, 1977]. The degree of relative political influence of hawks and doves in each of the societies depends in this model on two control parameters: the perceived cost of a war, b, and the fear of defeat, a. The state variable, x, is this degree of influence, or the governmental policy determined by it, ranging from peaceful ($x < 0$) to hostile ($x > 0$).

Arms races

A further application to the arms race of two nations suggests itself very naturally. The armament and hostility of one nation will surely affect both the fear of war and the cost of war within the other nation, and thus its armament level, and *vice versa* [Abraham, 1986]. It has been known that the strength of the peace movement in West Germany was crucial in supporting the forces which were essential in bringing M. Gorbachev to power, which in turn increased the influence of the peace movement in both parts of Germany. A slightly more complex configuration of political groups and their influence on decision making is discussed in Holsti & Rosenau [1988], in which the classification of the opinions in the population in foreign policy affairs are listed as: hardliners, internationalists, isolationists, and accomodationists.

Richardson

The response of a nation to the armament of another hostile nation has been subject to mathematical modeling of various types. Probably the first, and one of the best known, was introduced by L. F. Richardson in 1919 [Richardson, 1960a,b]. More recently these have been discussed in the framework of nonlineardynamical systems [Grossmann & Mayer-Kress, 1989;

Campbell & Mayer-Kress, 1989; Mayer-Kress, 1991] and genetic algorithms [Forrest & Mayer-Kress, 1990]. Other approaches have been based on mathematical game theory.[1] Game theory has also been used to model aspects of public opinion formation, which can then be fed back to the general sociological state of a nation [Axelrod, 1984].

Kadyrov

An application to the international relations of two nations, modeled by a coupled system of two cusps, or *double-cusp model*, was proposed by Kadyrov, in which the control parameters are the scaling factors of linear coupling functions from the state of one cusp to the controls of the other.[2] His model has a nongradient factor of one dimension. When this factor is set to zero, a special case of the gradient double-cusp catastrophe studied by Callahan and Sashin (of codimension eight) is obtained [Callahan & Sashin, 1987; Callahan, 1982]. We call this the *symmetric case*. Kadyrov studied the response diagram of the coupled scheme of the nongradient double cusp by simulation, discovering degenerate fold catastrophes, and the surprising periodic attractors we call *Kadyrov oscillations* [Kadyrov, 1984]. This oscillation is reminiscent of that found by Smale in the context of two coupled cells [Smale, 1976]. It may be useful in applications to situations of partnership or codependence, in which one wants to avoid a persistent state of repetition, a *vicious cycle*. Oscillations can occur in situations where strong polarization in one population is combined with a strong coupling to the dominant forces in the other country: Any transition to a new policy in the country X leads to an increased support of the opposition in country Y, which in turn leads to a transition to a new policy in country Y, which leads to an increased support of the opposition in the country X, which leads to a transition to a new policy in country X, etc. Our study was motivated by Kadyrov's paper, but we envision the double-cusp models as universal model families, applicable to a wider range of social dichotomies, such as competition and cooperation in the political and economical sectors.

Callahan and Sashin

A double-cusp model for anorexia and other psychological disorders has been studied by Callahan and Sashin.[3] This is a different kind of model, belonging to the context of elementary catastrophe theory. Our model, although sharing the same name, is a nongradient system. It has limit cycles, which do not occur in the gradient systems of catastrophe theory. Our model is similar to that of Callahan and Sashin in the special case which we call the *symmetric case*, mentioned above. But, in the more general case, our double-cusp models may still be applied to a wide variety of two-partner systems, as suggested by the work of Callahan and Sashin. Thus, applications may be envisioned to conflict resolution, cooperation, codependence, and so on.

Degeneracy

The response diagram obtained by Kadyrov appears degenerate, as its bifurcation curves involve two simultaneous bifurcation events, each known to be generically of codimension one. A generic codimension-one event has a bifurcation set, in the control space, of codimension one. Thus, in a two-dimensional control plane, the bifurcation set is a curve. Generically, two bifurcation curves should be transversal. That is, they should cross without tangency, or not at all. The coincidence of two bifurcation curves, each corresponding to a different bifurcation event, is thus very degenerate, or nongeneric. The modification of a scheme to remove such degeneracies is called *unfolding* the scheme.[4] We investigate the unfolding of the double cusp by computational means. The results of this investigation, described in the next three sections, are quite compatible with singularity theory. Further, in Sec. 6, we investigate a discrete-time analog of the double cusp, for which the critical point solutions can be found analytically, looking forward to computational economies in future work with several coupled cusps [Abraham, 1990]. For this discrete scheme, we find an equivalent unfolding and response diagram. We also find more complex solutions which are excluded in the continuous model, namely bifurcations to quasiperiodic, and also chaotic, solutions. In the conclusion, we speculate on some directions for future work.

2. Two-Cusp Catastrophes, Continuous-time, Kadyrov Style

We will adopt the notations of the Isnard and Zeeman model for hawks and doves [Isnard & Zeeman, 1977].

[1] See, for example, Brams [1985] and Wendroff [1990].
[2] The Russian original is Kadyrov [1984]. As this may be difficult to find, we would be happy to send copies of this paper, in the original Russian, or in an informal, English translation.
[3] All of the relevant papers are found in the list of references, see especially Callahan [1982].
[4] See any text on Catastrophe Theory, e.g., Poston [1978].

Although a bit different from the usual notations of catastrophe theory, this is compatible with Kadyrov. Let

$$\phi(x, a, b) = -\frac{1}{4}x^4 + \frac{b}{2}x^2 + ax$$

where ϕ is a real-valued function of three real variables, and ϕ_x denotes the partial derivative with respect to x. Recall that in the language of complex-dynamical-systems theory, a dynamical scheme is a dynamical system depending upon control parameters.[5] The dynamical scheme of the cusp is

$$x' = \phi_x(x, a, b) = -x^3 + bx + a$$

with the familiar response diagram shown in Fig. 1 (taken from Isnard and Zeeman, Fig. 11). The control parameter a is called the *normal factor*, and controls the overall height of the graph, G, or bias. The control parameter b is called the *splitting factor*, and it controls the spread between the two layers of the fold. In the application of Isnard and Zeeman to opinion formation in a democratic nation, the splitting factor represents the depth of the split in public opinion between the two segments of the population.

In the spirit of complex-dynamical-systems theory, we may couple two cusps in a minimal network. Each of the control parameters of one of the cusps may be expressed as a function of the state of the other. We consider in this section only one special case, that of Kadyrov's two-nation model [Kadyrov, 1984; Abraham, 1987]. Thus, we let the normal factor of each be proportional to the state of the other. Then the scheme is described by the system of two ordinary differential equations:

$$x' = -x^3 + bx + ay \ ,$$

$$y' = -y^3 + dy + cx \ .$$

Here, ay has replaced a as the normal factor of the x cusp. Thus, in the context of Kadyrov's application, the normal factor (height or bias) within each nation is proportional to the state (armament level) of the other nation. The parameter b retains its significance as the splitting factor. Rhyming notations have been chosen for the y cusp, in place of the letters used by Kadyrov.

These equations define a dynamical scheme with two-dimensional state space, $(x, y) \in R^2$, and four-dimensional control space, $(a, b, c, d) \in R^4$. Due to the source of this dynamical scheme within elementary catastrophe theory (ECT), we may expect this to be a *gradient system* [that is, the gradient of a function, $\phi(x, y)$]. In general, it is not, for the partial derivative of the x' function with respect to y is a, while that of the y' function with respect to x is c.

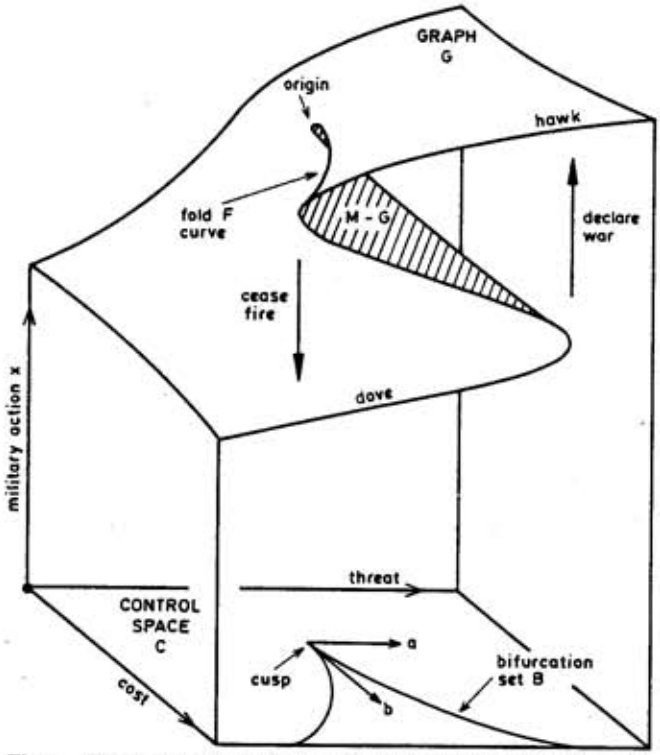

Fig. 1. The cusp catastrophe of ECT, from Isnard and Zeeman, Fig. 11.

Thus, in the *symmetric case*, in which $a = c$, the coupled system is a gradient scheme with three-dimensional control (that is, the gradient of a potential function of two variables, depending upon three control parameters), equivalent to one of the standard catastrophes of ECT.[6] Its potential function is

$$\phi(x, y) = -\frac{1}{4}(x^4 + y^4) + \frac{1}{2}bx^2 + axy + \frac{1}{2}dy^2 \ .$$

Its bifurcation set is an algebraic surface in R^3.

But in the general, *asymmetric* case, we have a non-ECT response diagram. The asymmetry may be interpreted, in Kadyrov's application, as a difference between the nations in response to the same stimulus, perhaps due to paranoia. Kadyrov has obtained, for example, the section of the bifurcation set shown in Fig. 2, where (b, d) has been chosen in the *Kadyrov*

[5]For definitions, see Abraham [1987].
[6]See p. 185 of Poston [1978] for a discussion of umbilics.

wedge, that is, such that $b > 2d$ and $d > 2b$ (adapted from Kadyrov, Fig. 6). In Kadyrov's context, such an oscillation represents a potentially undesirable situation, in which the two nations take turns increasing, then decreasing, their armaments, a costly and wasteful scenario. In a context of codependence, such as Callahan and Sashin have studied, the oscillation may be a model for a cycle of indulgence and withdrawal. The cusps represent fold catastrophes as before, while the parabolic curves represent blue-loop explosions.[7] We may explain these in more detail by considering phase portraits in the four distinct regimes of the sections (A through D) in Fig. 2. Some corresponding phase portraits are shown in Fig. 3. The jargon from bifurcation theory may be found in *Part Four* of Abraham [1982–88].

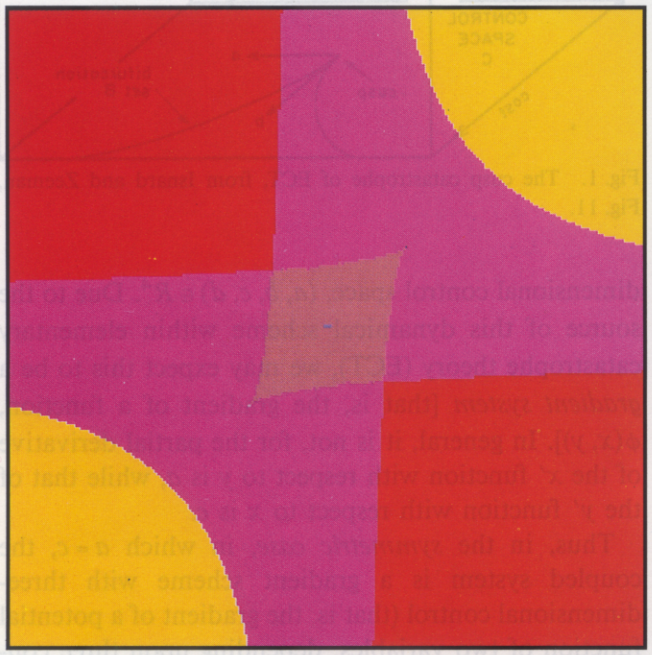

Fig. 2. The bifurcation set of the double cusp, from Kadyrov, Fig. 6. The colors indicate the number of fixed points at a given parameter combination: red = 1, yellow = 3, purple = 5, brown = 9 fixed points. Note that due to degeneracy there are no regions with 7 fixed points.

(A) In the central region enclosed by the two cusps, there are four static nodal attractors (one in each quadrant, I, II, III, and IV), four saddles (their insets comprising the separators of the four basins), and one central nodal repellor.

(B) Here there are two point attractors (in quadrants I and III), two saddles, and one central repellor. Across the bifurcation curve between A and B there are two fold catastrophes, in each of which a point attractor and a saddle mutually annihilate. (If nondegenerate, these would occur one at a time across disjoint curves.)

(C) Two attractors as in B, but across the bifurcation curve between B and C there is a fold in which one saddle and the central repellor annihilate. This is a basin bifurcation. That is, the net effect of the event is a sharp change in the partition of the state space into basins.

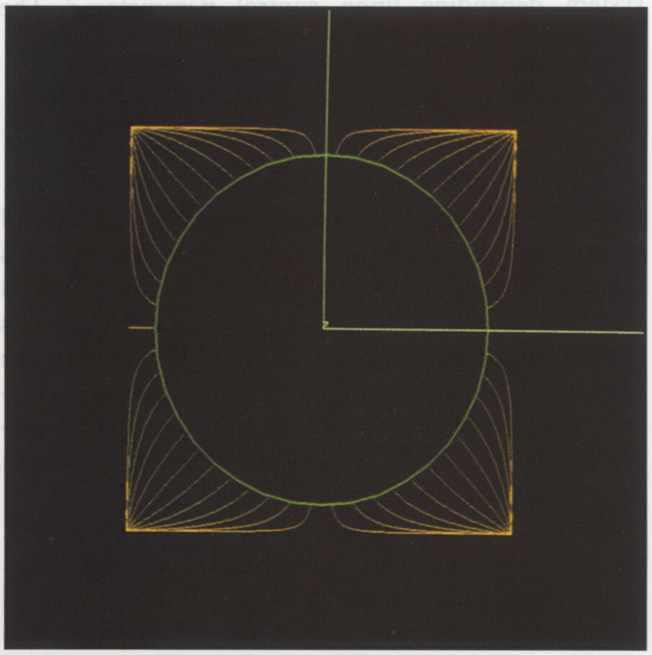

Fig. 3a

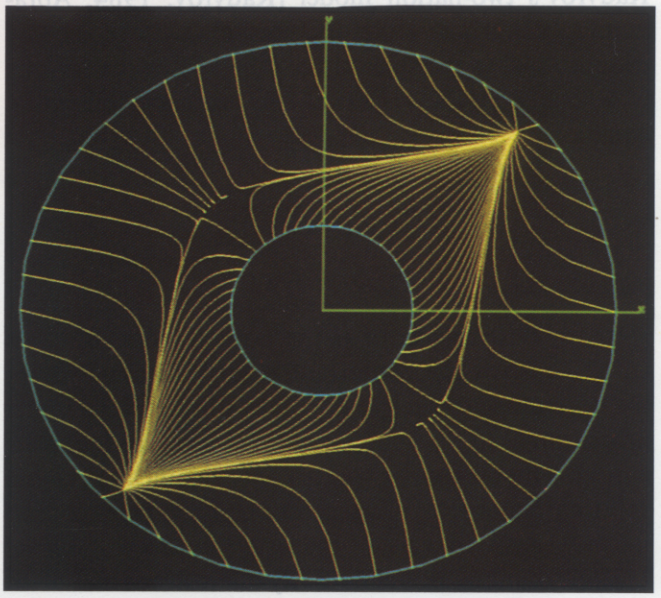

Fig. 3b

[7] In the blue-loop, an attractor and a saddle point annihilate, exploding into a periodic attractor. In other words, this is a saddle-node bifurcation within the outset of the saddle. See Sec. 6.1 of *Part Four* of Abraham [1982–88].

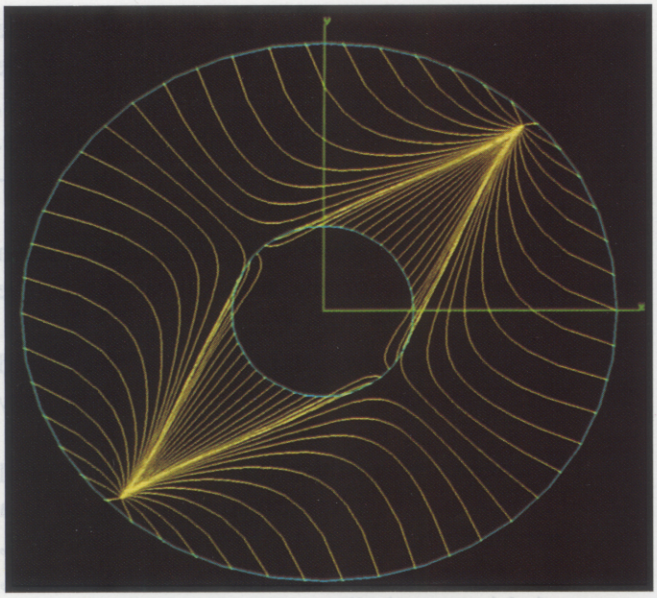

Fig. 3c

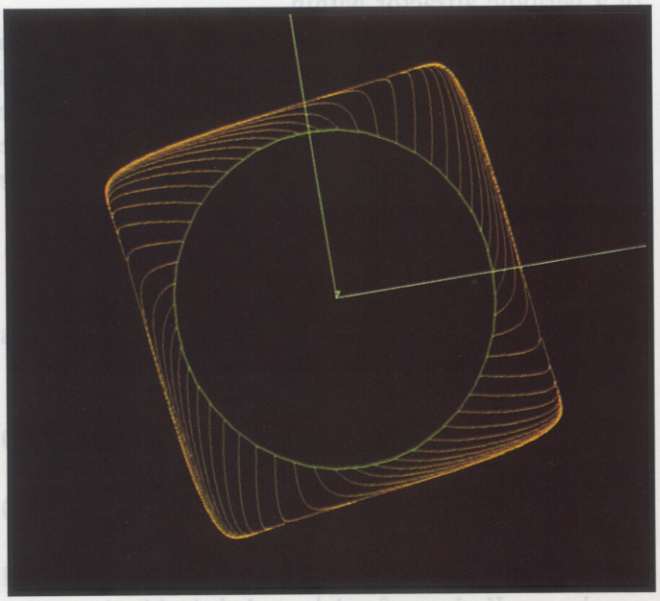

Fig. 3d

Fig. 3. Phase portraits showing the transition from a multiple fixed point to a Kadyrov oscillator. In all Fig. 3 plots, $b = d = 1$. Initial conditions are chosen on two concentric circles in the basin of the attractors: 50 trajectories on the outer circle and 30 on the inner.

(a) Plot with $a = c = 0.1$. Here we see 9 critical points: 4 attractive, 4 hyperbolic, and $(x, y) = (0, 0)$ is a repellor.

(b) Plot with $a = c = 0.5$. Here we see 5 critical points: 2 attractive, 2 hyperbolic, and $(x, y) = (0, 0)$ is still a repellor.

(c) Plot with $a = c = 1.0$. Here we see 3 critical points: 2 attractive and $(x, y) = (0, 0)$ is a hyperbolic saddle point.

(d) Plot with $a = 1.0$ and $c = -1.0$. We have an attractive periodic solution: a Kadyrov oscillator.

(D) In this regime there is a single attractor (periodic) and a central spiral repellor. Across the bifurcation curve separating B (or D) from E, there is a degenerate blue-loop explosion, in which both point attractors (in B or D) explode simultaneously. (In a nondegenerate analogue, each blue-loop event would occur across its own distinct curve. Alternatively, there might be a fold catastrophe, followed by a single nondegenerate blue-loop.) We call the attractor a *Kadyrov oscillator.*

The degeneracy apparent in Fig. 2 consists in the multiple bifurcations from four attractors (static) to two attractors (static), and from two attractors (static) to one attractor (periodic) across a single bifurcation curve in the control plane. In the next section we will *unfold* the system, by adding control parameters to obtain a sequence of bifurcation curves, across which the four attractors change to three, to two (each time by a fold catastrophe) and finally to one (by a blue-loop explosion). The dependence of the (a, c) section upon the other two controls, (b, d), is indicated in the tableau of Fig. 4. These critical-point maps have been computed by Newton's method, applied to the appropriate polynomial function (see Sec. 5).

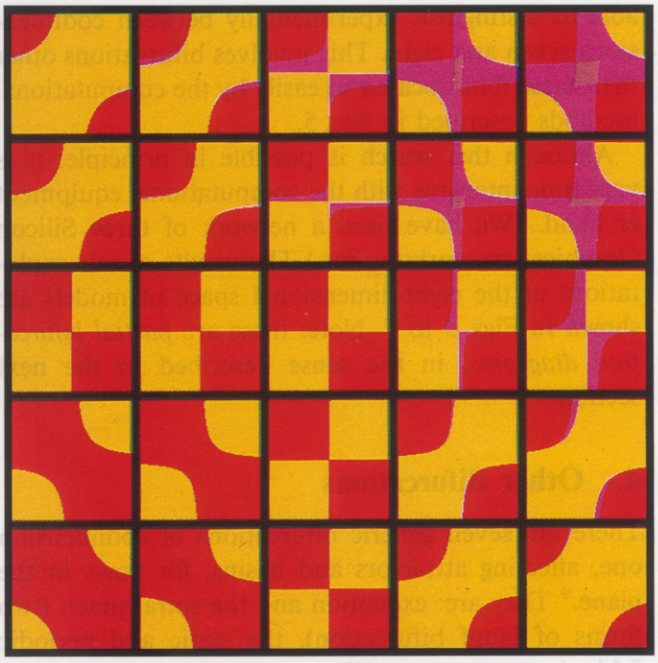

Fig. 4. A four-dimensional portion of the bifurcation set belonging to Kadyrov's model. We represent the parameters a, c as dimensions in a tableau of small squares. The position of each small square defines a location in the (b, d) subspace. The same representation has been chosen in Figs. 7 and 14–19. Note: The upper right square $[(b, d) = (1,1)]$ is a reproduction of Kadyrov's Figure 6. In all small squares, (a, c) range from -2 to $+2$. (Same color coding as in Fig. 2).

3. Two-Cusp Catastrophes, Continuous-Time, Unfolded

Recall that the Kadyrov scheme is described by the system of two ordinary differential equations:

$$x' = -x^3 + bx + ay \ ,$$

$$y' = -y^3 + dy + cx \ .$$

We now attempt to unfold this by adding terms suggested by elementary catastrophe theory. Thus, we will study the scheme:

$$x' = -x^3 + (b_0 + b_1 y)x + (a_0 + a_1 y) \ ,$$

$$y' = -y^3 + (d_0 + d_1 x)y + (c_0 + c_1 x) \ .$$

Terms in x^2y and xy^2 have been omitted, as singularity theory suggests their relevance for unfolding under differentiable equivalence only.[8] Lacking a suitable theory, we seek to establish the completeness of this scheme by computer simulation. The main goal of this paper is to report the results of these simulations, which do suggest that this scheme is a generic family of dynamical systems, transversal to a bifurcation stratum of codimension eight. Actually, we are not able to distinguish experimentally between codimensions seven and eight. This involves bifurcations other than these folds located so easily by the computational methods described in Sec. 5.

Although this search is possible in principle, it is very time intensive with the computational equipment at hand. (We have used a network of three Silicon Graphics Iris workstations.) The results of our explorations of the eight-dimensional space of models are shown in Figs. 5 to 7. Note: these are *partial bifurcation diagrams*, in the sense described in the next section.

4. Other Bifurcations

There are seven generic bifurcations of codimension one, affecting attractors and basins, for flows in the plane.[9] They are: excitation and the spiral pinch (two forms of Hopf bifurcation), the static and periodic folds (appearance or disappearance of an attractor along with its separator), basin bifurcation (change in a basin or separator only), the periodic blue sky (a periodic attractor appears out of the blue), and the blue loop (through a fold on an invariant cycle, a saddle-connection becomes a periodic attractor). We believe that *all seven occur* in our unfolded scheme. Thus, the response diagrams presented in the preceding section, showing fold and blue-loop curves only, are incomplete. Although we have not yet located them in our simulations, we might expect the following.

a. For a_0 and c_0 outside Kadyrov's wedge, excitation may occur for some of the static attractors in the regimes of two to four attractors.

b. For b_0 and d_0 in the distant corners of the second and fourth quadrants, the Kadyrov oscillation may vanish in a periodic blue-sky catastrophe.

c. For some values of the eight controls, the central static repellor may be transformed from a node to a focus (not a bifurcation), and then undergo excitation, producing a central static attractor of spiral type, surrounded by a periodic repellor. A nearby periodic fold (cusp style) will then create a small annulus bounded by two periodic repellors, which is the basin of a periodic attractor within.

d. In addition to these, there may also be basin bifurcation curves. That is, as the parameters cross these curves in the bifurcation diagram, a saddle connection forms momentarily, as the outset of one saddle (which separates two basins) sweeps past the inset of another saddle.

5. Critical-Point Analysis

We began our investigation by reproducing Kadyrov's Figure 6. This figure is an a_1–c_1 cross-section, where

$$x' = x^3 + (b_0 + b_1 y)x + (a_0 + a_1 y) \qquad (1)$$

$$y' = y^3 + (d_0 + d_1 x)y + (c_0 + c_1 x) \qquad (2)$$

and the "non-Kadyrov" variables: b_1, d_1, a_0, and c_0 all equal zero. Kadyrov fixed b_0 and d_0 inside the wedge defined by $b_0 < 2d_0$ and $d_0 < 2b_0$.

To reproduce Kadyrov's Figure 6, we need only calculate the number of critical points as a function of the parameters. We find the critical points of the system by finding all (x, y) pairs such that

$$0 = x^3 + (b_0 + b_1 y)x + (a_0 + a_1 y) \quad \text{and} \qquad (3)$$

$$0 = y^3 + (d_0 + d_1 x)x + (c_0 + c_1 x) \ . \qquad (4)$$

Solving (3) for y and substituting into (4), we can determine the number of critical points as the number

[8] See Callahan [1987] for example, and the references therein.
[9] See Secs. 2.1, 3.2, 3.3, 4.1, 5.1, 5.2, and 6.1 in *Part Four* of Abraham [1982–88].

Fig. 5. A blowup of the central region of our unfolded version of Kadyrov 's Figure 6. Same as Fig. 4, but now the non-Kadyrov term is $b_1 = 0.1$. Note: The algorithm used when $|c_0| < 0.3$ is different from the algorithm used elsewhere. Due to convergence considerations, we solve Eq. (4) for x first and then substitute into Eq. (3).

The three horizontal rows of pixels across the center of the cross-section are caused by convergence problems or similar numerical artifacts.

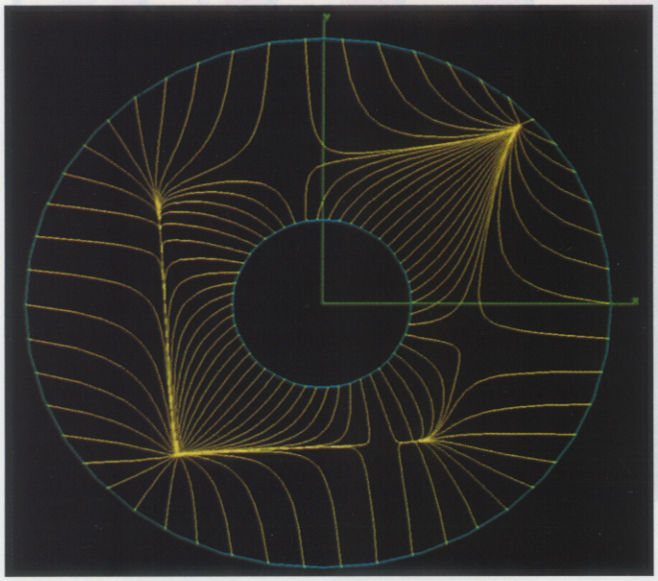

Fig. 6. Phase portrait for Fig. 5, region of seven critical points.

of real roots of a ninth-order polynomial. We designate this polynomial, $f_c(x)$, the *critical point function*. Particularly near $(b_1, d_1, a_0, c_0) = (0, 0, 0, 0)$, the critical-point function clearly shows the number of system critical points produced by this parameter setting, see Fig. 8.

This critical-point function is very useful in determining the bifurcation curves. For example, in Fig. 9, there appears to be a region (B), corresponding to five critical points, which has opened up in the midst of a region (A, C) corresponding to three critical points. Wondering whether the appearance of this region corresponded to the appearance of two (saddle) critical points, we examined phase portraits for these parameter settings. We found it difficult to determine whether these saddle points are there or not in this manner. Yet, inspection of the graph of $f_c(x)$ in these parameter regions shows that two saddle points do form briefly, and we can immediately determine the x-coordinates of these critical points. (See Figs. 10a, 10b, and 10c).

It is important to note that we will always be able to form such a function from a system of connected cusp models as long as we limit ourselves to linear coupling. Thus, this function could be a very important tool in locating precisely much of the bifurcation set of such a model.

6. Two-Cusp Models with Discrete Time

The interesting properties of the cusp models described above are given by the bifurcation behavior under changes of control parameters. For a single cusp the bifurcations are between solutions with one or three critical points. In the discussion in Secs. 1 through 4 we have used models defined by ordinary differential equations (ODEs). The equivalent dynamical behavior can also be modeled with the help of diffeomorphisms f: $R \to R$, inducing a discrete-time evolution of a state variable $x \in R$ through $x_{n+1} = f(x_n)$, where $n \in Z$ indicates a discrete-time variable. This method has already been used in the context of reaction–diffusion models (see, for example, Keeler [1987]) and models for phase transitions [Oono & Yeung, 1987; Oono & Puri, 1986]. Its advantages are better analytical accessibility, a large reduction of numerical problems, and a dramatic increase in computational speed.

In order to model a single cusp we define for a, $b \in R$, $b > 0$, the family $f(x, a, b) = \tanh(bx) + a$ (see Fig. 11). As in the ODE case we have a splitting parameter, b, and a normal parameter, a. For $b < 1$, the slope of $f(x, a, b)$ is everywhere less than one, and therefore there exists only one fixed point, x_c [that is, $f(x_c, a, b) = x_c$], and this is always stable and globally attracting. The location of x_c is determined by the values of both a and b.

Now increase b, keeping $a = 0$. Since $f'(0, a, b) = b$, the fixed point x_c becomes unstable for $b = 1$. Simultaneously, two new fixed points ($x_l \leq x_c \leq x_r$) are created.

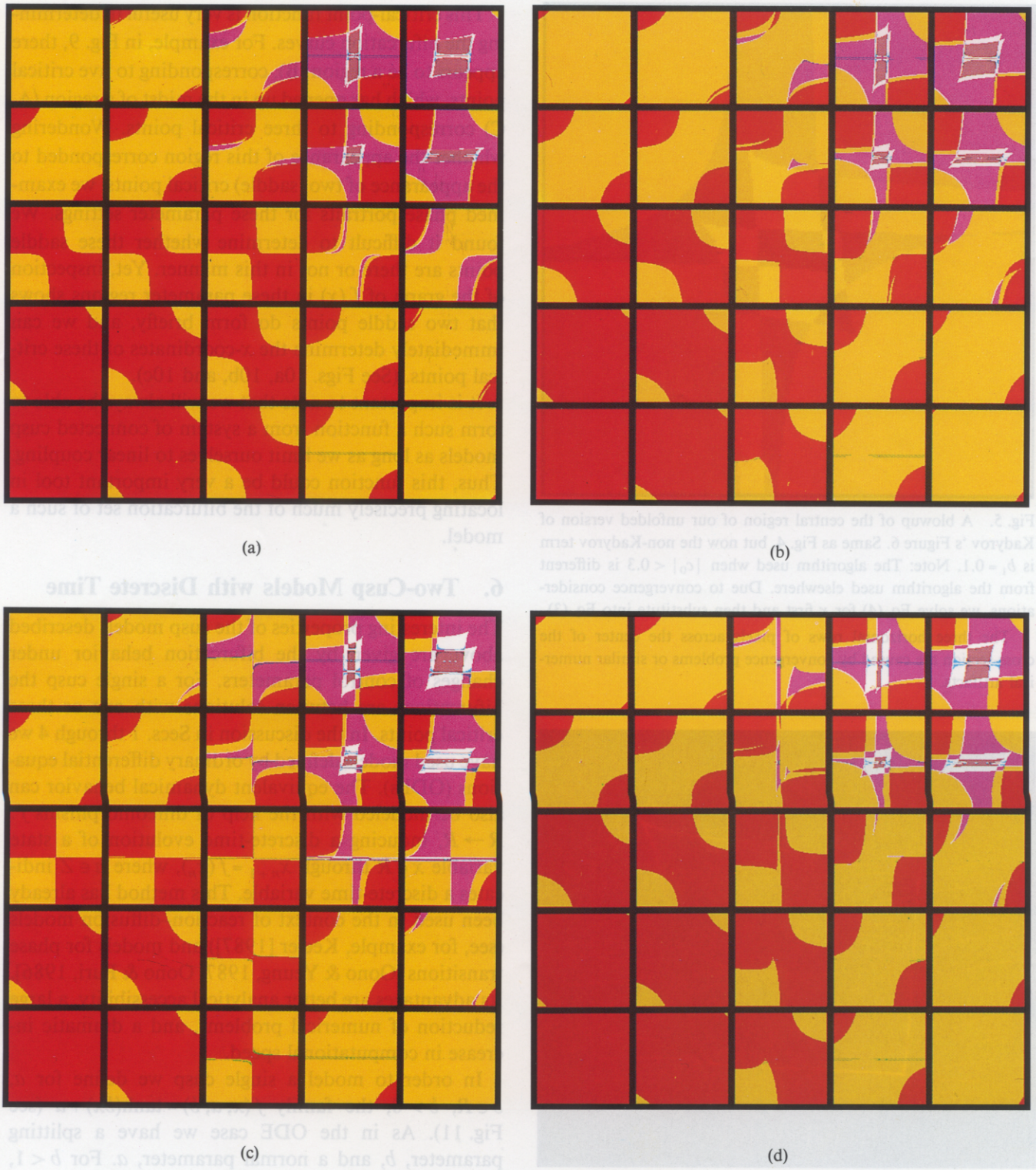

Fig. 7. Tableaus for other values of the parameters (same color code as in Fig. 2). (a) The non-Kadyrov parameter appearing in the normal factor of nation X, a_0, has been changed from $a_0 = 0.0$ to $a_0 = 0.1$. Notice the thin regions in the upper right cross-section corresponding to 3 (resp. 7) critical points which is opening between the regions corresponding to 1 (5) and 5 (9) critical points. Color code as in Fig. 2. (b) Further unfolding as the non-Kadyrov parameter appearing in the normal factor of nation Y, c_0 is increased from 0.0 to 0.2. (c) The unfolding which takes place as both non-Kadyrov variables appearing in the splitting factors of each nation, b_1, d_1, are changed to $b_1 = 0.1$, $d_1 = 0.2$. Compare with Fig. 7b, where the non-Kadyrov variables appearing in the normal factors (a_0, c_0) of each nation were changed by the same amount. (d) Here, the non-Kadyrov variables appearing in both the normal and the splitting factors of nation X, b_1, and a_0, have been changed to values of $a_0 = 0.1$, $d_1 = 0.2$.

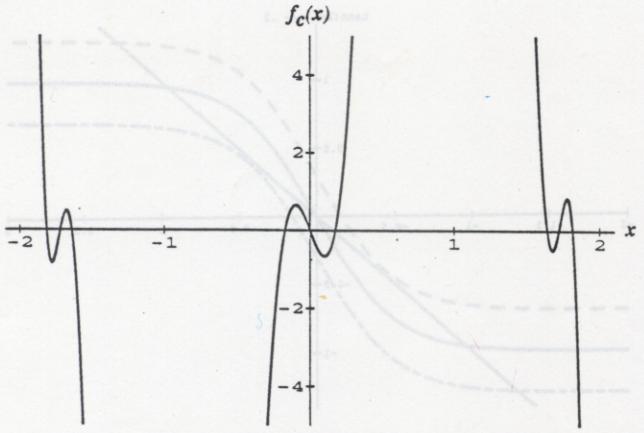

Fig. 8. The graph of the critical point function, $f_c(x)$, at the specified parameters. Notice this setting of the parameters occurs within a region corresponding to 9 critical points: one unstable critical point at the origin, four stable critical points, and four saddles.

They are stable since $f'(x, a, b) \to 0$ for $x \to \pm\infty$ and f is invertible. The degeneracy of the simultaneous creation of x_l and x_r can be unfolded by allowing $a \neq 0$. The bifurcation from solutions of one fixed point to those with three fixed points is of fold (saddle-node) type, and corresponds to the fold in the ODE case. For any value of $b > 1$ we can find $a_s \neq 0$ such that the system undergoes a saddle-node bifurcation at (a_s, b). We observe that for all $a \in R$, $b > 1$, for which we have three fixed points, x_l and x_r are stable, while x_c unstable. For $a > 0$ we have $x_c < 0$ and for increasing a, x_l and x_c will coalesce and disappear in a fold bifurcation. Analogously for $a < 0$, x_c and x_r will disappear. From the construction, we see that approach to the stable fixed points x_l and x_r is always monotone, and that the rates ($|f(x, a, b) - x|$) at which the fixed points are approached goes to infinity for $|x| \to \pm\infty$. This is an important difference from the cubic functions studied by R. Kapral, which exhibit a much more complex bifurcation structure [Kapral, 1985, 1986]. His cubic functions can have multiple critical points and therefore are not invertible, which means that they cannot be viewed as Poincaré maps of ODEs. Thus, the solutions can overshoot, and show many artifacts, as in the Euler integration of nonlinear ODEs. Using our map, we have excluded the occurrence of such spurious solutions. But in order to guarantee that the numerical solution shows the correct qualitative behavior, for example, conservation of symmetries, careful implementation is required.

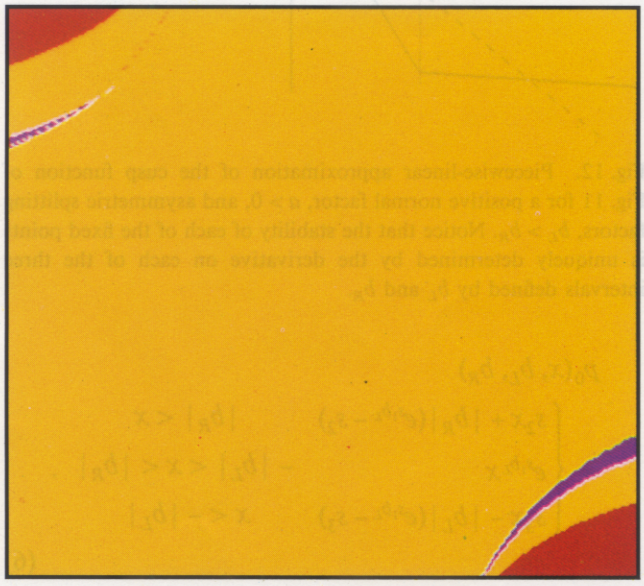

Fig. 9. An interesting cross-section (a_1, c_1) of the parameter space for $a_0 = 0$, $c_0 = 0$, $b_0 = -1.0$, $d_0 = 2.0$, $b_1 = 0.1$, $d_1 = 0.2$. Parameter points in the lower right corner generate the critical point function, $f_c(x)$, shown in Fig. 10a,b,c. See discussion following Eq. (4). Same color code as in Fig. 2.

The eigenvalues of the fixed point, i.e., their local stability properties as well as their separation, are determined both by the splitting parameter b and the normal parameter a. We also see that this system has strong symmetry properties, which suggest nongeneric behavior. In order to introduce a controlled and interpretable symmetry-breaking condition for the generic unfolding of the coupled-cusp system, and also in order to be able to find the fixed points analytically, we introduce a continuous, piecewise-linear function, $p(x, a, b_L, b_R)$, with a set of solutions equivalent to the hyperbolic tangent map $f(x, a, b)$.

The map $p(x, a, b_L, b_R)$ consists of three linear parts, each determined by parameters specifying slopes and y-intercept, determined by (b_L, b_R), of the local linear segment. Whereas the relative location of the three pieces with respect to each other controls the bifurcation set, the local slopes permit explicit control

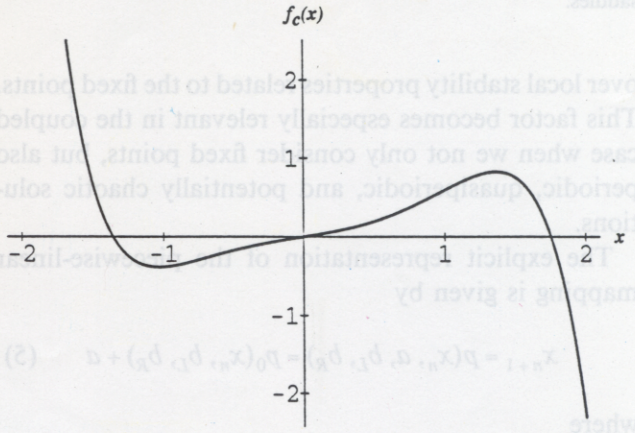

Fig. 10a

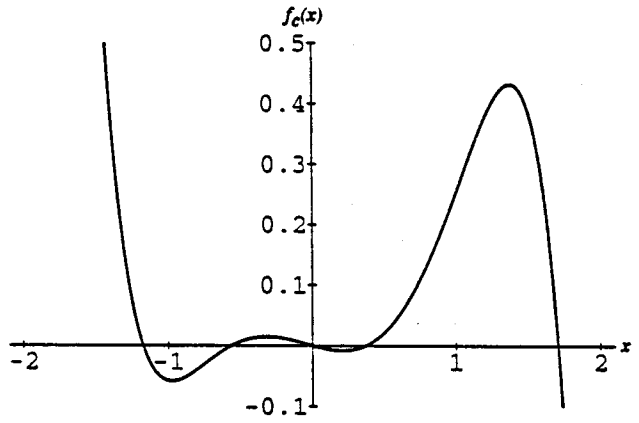

Fig. 10b

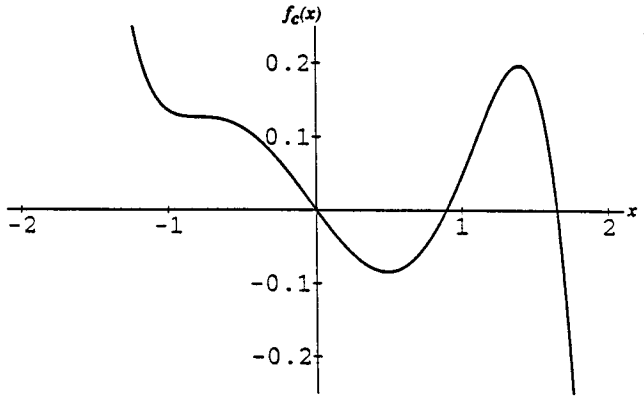

Fig. 10c

Fig. 10. Graphs of the critical point function f_c [see discussion following Eq. (4)]. (a) Graph of $f_c(x)$ at a point in the large yellow region of Fig. 9 close to the purple region. From phase space analysis, it is known that the critical point at $(a_1, c_1) = (0, 0)$ is a repellor and the other two critical points are attractors. (b) Graph of $f_c(x)$ in the purple region in the lower right corner of Fig. 9, showing the appearance of the two saddles and leading to 5 coexisting fixed points. (c) Graph of $f_c(x)$ in the yellow region between the purple and the red region in the lower right corner of Fig. 9, showing that the system has returned to 3 critical points. Notice that now, however, one of the attractors has disappeared along with one of the saddles.

over local stability properties related to the fixed points. This factor becomes especially relevant in the coupled case when we not only consider fixed points, but also periodic, quasiperiodic, and potentially chaotic solutions.

The explicit representation of the piecewise-linear mapping is given by

$$x_{n+1} = p(x_n, a, b_L, b_R) = p_0(x_n, b_L, b_R) + a \qquad (5)$$

where

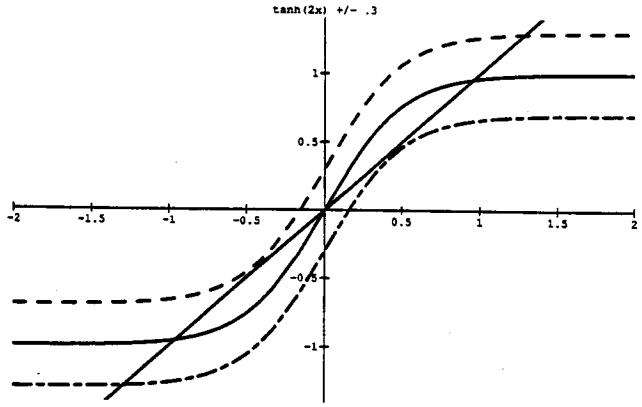

Fig. 11. Graph of $f(x, a, b) = \tanh(bx) + a$ as a discrete version of a cusp model (in the figure we have a splitting factor $b = 2$). The symmetric case is given by normal factor $a = 0$ (solid line) with an unstable fixed point at the origin and two symmetric, stable fixed points. For a positive value of the normal factor a only the stable fixed point at positive x-values remains ($a = 0.3$ dashed line), for negative values of the normal factor a the situation is reversed ($a = -0.3$, dot-dashed line).

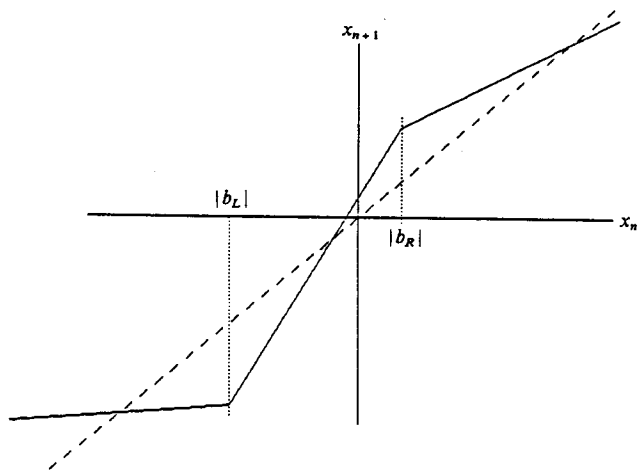

Fig. 12. Piecewise-linear approximation of the cusp function of Fig. 11 for a positive normal factor, $a > 0$, and asymmetric splitting factors, $b_L > b_R$. Notice that the stability of each of the fixed points is uniquely determined by the derivative on each of the three intervals defined by b_L and b_R.

$$p_0(x, b_L, b_R) = \begin{cases} s_2 x + |b_R|(e^{s_1 b_L} - s_2) & |b_R| < x \\ e^{s_1 b_L} x & -|b_L| < x < |b_R| \\ s_3 x - |b_L|(e^{s_1 b_L} - s_3) & x < -|b_L| \end{cases} . \qquad (6)$$

Here b_L and b_R play the role of the splitting factor, and a plays the role of the normal factor, of the continuous-time model studied above. For a positive values of b_L and a, the mapping is shown in Fig. 12.

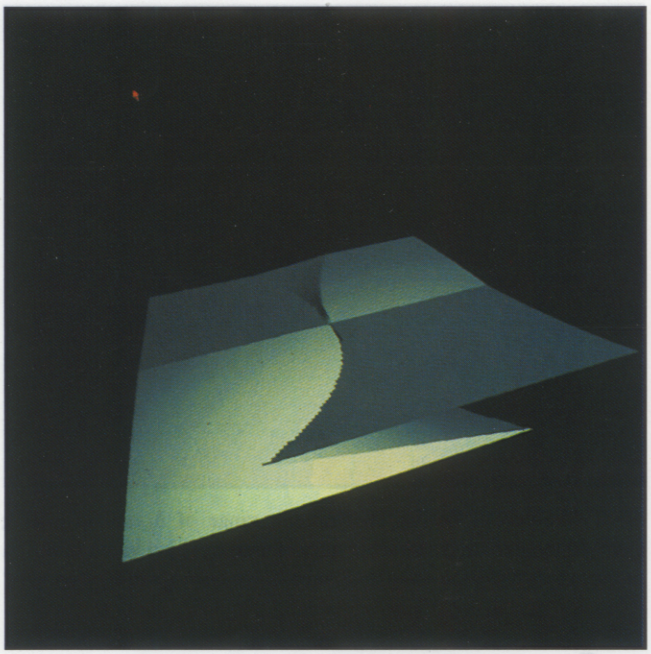

Fig. 13. The cusp surface for the piecewise-linear cusp function, $p(x, a, b_L, b_R)$ of Fig. 12, where $b_L = b_R$. Same representation of the control and state space as in Fig. 1. Notice that most of the bifurcation structure is concentrated in the upper right corner of the tableau, corresponding to large values of b_L and d_L.

Figure 13 displays the cusp surface obtained from the above mapping. As the splitting factor, b, changes from a negative to a positive value, it is evident that the central region of this mapping displays the divergence and inaccessibility characteristics of the standard cusp catastrophe.

We now make the generalization to the two-nation model with the state of one nation, x, and the state of the other nation, y. The change of state of both nations is represented by iteration of the following map:

$$x_{n+1} = p_0(x_n, b_L, b_R) + a_1 y_n + a_0 \ , \qquad (7)$$

$$y_{n+1} = p_0(y_n, d_L, d_R) + c_1 x_n + c_0 \ . \qquad (8)$$

As in the ODE case, coupling is achieved through the normal factors. Solving analytically for the fixed points of this mapping, we are able to obtain a tableau of the dependence of the mapping on the control parameters. In Figs. 14 through 23, this dependence is shown as (a_1, c_1) slices within a (b_L, d_L) space, as in Fig. 14. Because we are able to solve for the fixed points analytically, we can resolve the numerical convergence problem visible in Fig. 5. Furthermore, because this mapping allows for symmetry breaking via b_R and b_L, we are able to resolve an additional direction of unfolding. However, at this time, coupling through the splitting factors has not been explored.

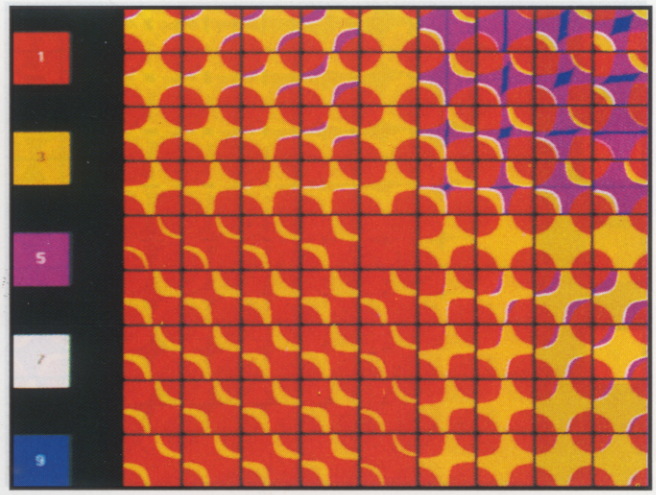

Fig. 14. The tableau for the symmetric case where $b_L = b_R$ and $d_L = d_R$, with the unfolding parameters $a_0 = c_0 = 0.0$. This is analogous to Kadyrov's continuous-time model, shown in Fig. 5. The domain of both b_L and d_L is $(-2, 2)$ at intervals of 0.5. Each a_1, c_1 slice is of the same domain, with a resolution of 0.02. The slopes (s_1, s_2 and s_3) for both nations are set to 0.5. (Same color code as in Fig. 2, except that nine fixed points correspond to a blue region.)

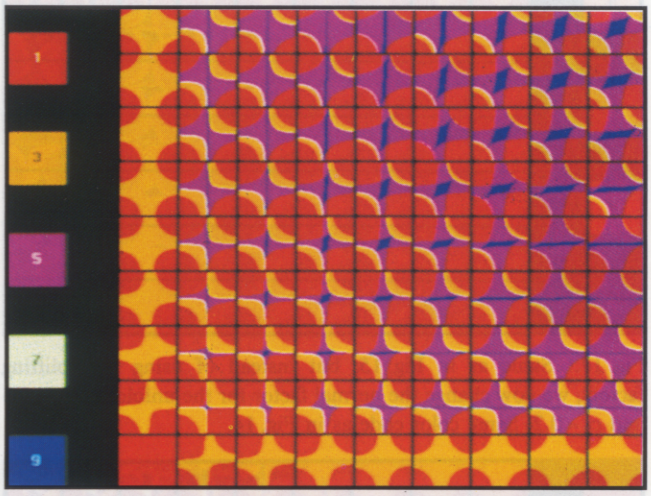

Fig. 15. Upper right quadrant of Fig. 14, with b_L, d_L in (0,2) and a_1 and c_1 unchanged. Same color code as in Fig. 14.

Investigating the phase portrait of this mapping for the symmetric case where $a_0 = c_0 = 0$, $b_R = b_L$ and $d_R - d_L$, we find much of the same behavior as found in the continuous model. Figure 20 displays the analogous phase portrait found in the regime of section F of Fig. 3 where there exist two point attractors, two saddles and one central repellor. In Fig. 21, we show the existence of the periodic attractor of period twelve found in the regime of section F. We also find that in increasing the slopes of the discrete mapping from 0.5 to 0.8, the periodic attractor changes to the quasi-periodic attractor of Fig. 22. In Fig. 23, we were able

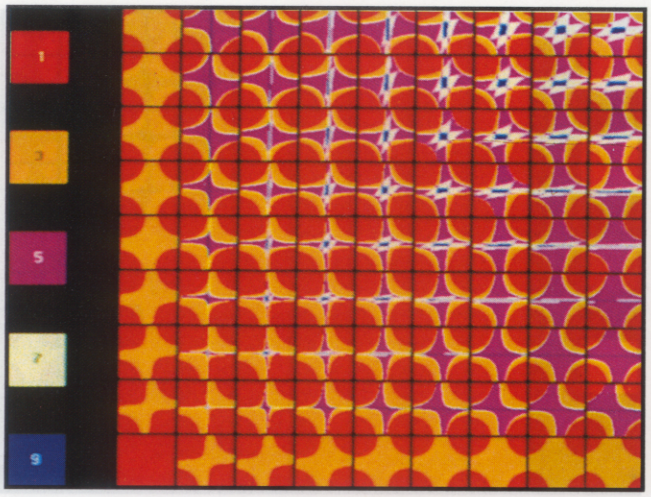

Fig. 16. Figure 15 with $b_R = 0.8 \cdot b_L$ and $d_R = 0.4 \cdot d_L$. Note the unfolding in the bifurcation sets associated with 5, 7, and 9 fixed points. Same color code as in Fig. 14.

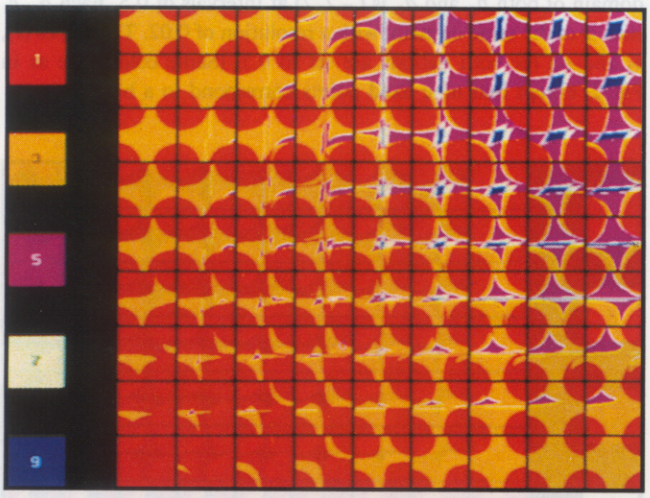

Fig. 17. Same as in Fig. 15, but instead of using the splitting factors, we now change the normal factor for the unfolding, $a_0 = 0.5$ and $c_0 = 0.2$. Same color code as in Fig. 14.

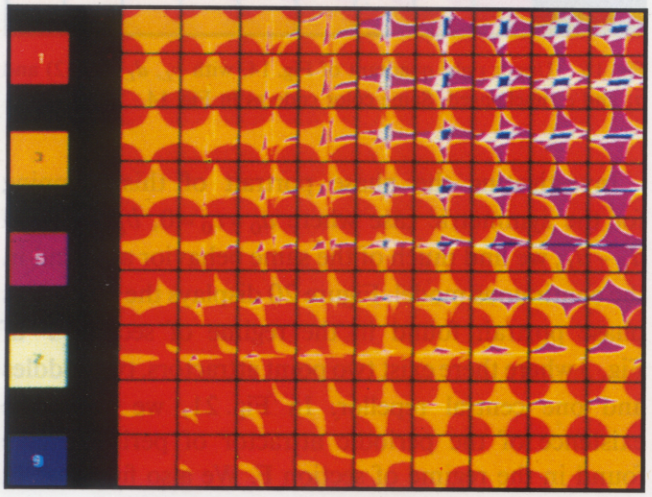

Fig. 18. Combination of the perturbations of the normal factor (as in Fig. 17) and the splitting factor, $b_R = 0.8 \cdot b_L$ and $d_R = 0.4 \cdot d_L$ as in Fig. 16. Same color code as in Fig. 14.

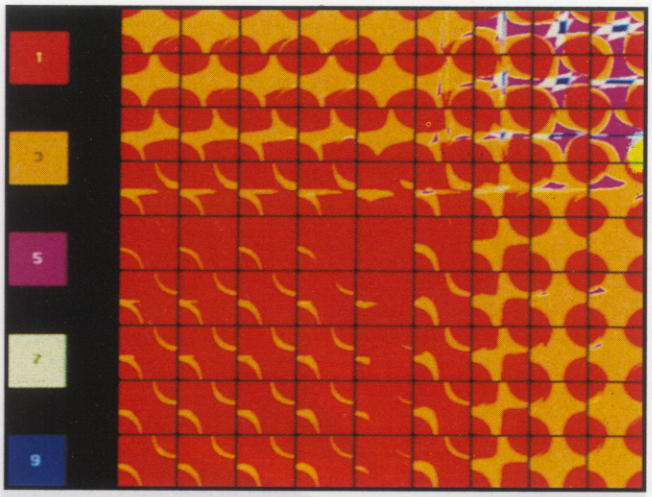

Fig. 19. Same as in Fig. 18 with the range of b_L and d_L being changed to $(-2, 2)$. Each subgraph is separated by a value of 0.5 in the splitting factors b_R and b_L. Same color code as in Fig. 14.

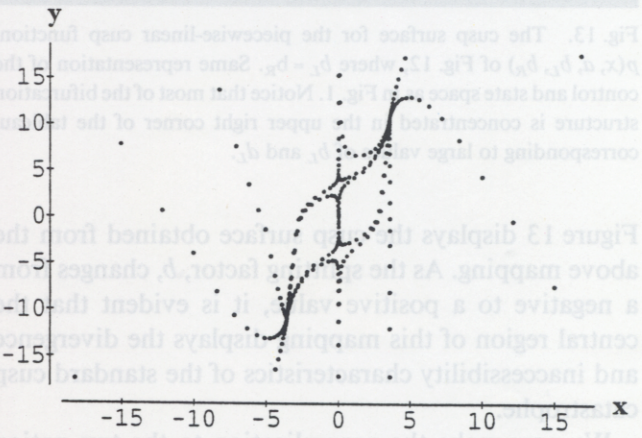

Fig. 20. Phase portrait of symmetric case for $a_1 = 0$, $c_1 = 0.5$, $b_L = 1.0$ and $d_L = 1.0$, a region of five fixed points: two attractors, two saddle points, and a central repellor.

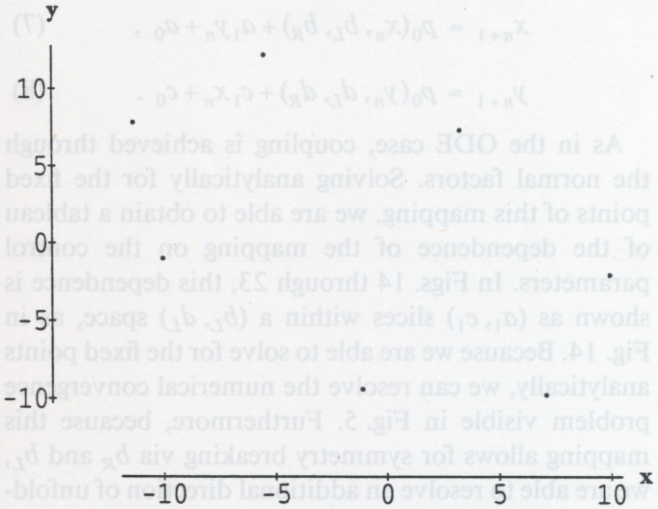

Fig. 21. Phase portrait of symmetric case for $a_1 = -0.5$, $c_1 = 0.5$, $b_L = 1.0$ and $d_L = 1.0$, a region displaying a periodic attractor.

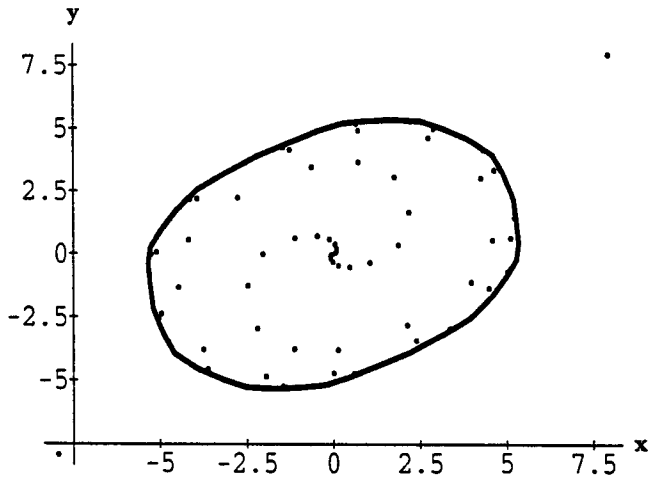

Fig. 22. The same conditions found in Fig. 21, but with the slopes of both nations increased to 0.8, display the existence of a quasi-periodic attractor.

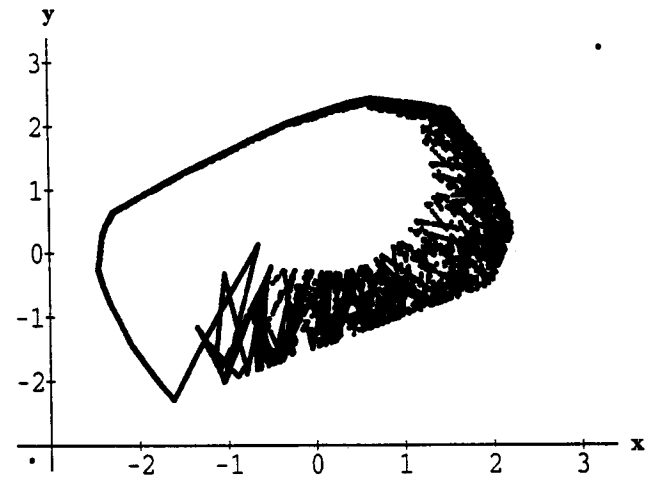

Fig. 23. The chaotic attractor found in the same region of Figs. 21 and 22, with all slopes equal to 0.5, except for s_3 of nation Y, which has a value of -1.5.

to find chaos, something not present in the ODE case as guaranteed by the Poincaré–Bendixson theorem. The existence of chaos in this case is generated through the local separation of nearby orbits, which is caused by those sections of the function, $p_0(x_n, b_L, b_R)$ with $|p_0'(x_n, b_L, b_R)| > 1$. The global boundedness of the system is guaranteed by those sections of $p_0(x_n, b_L, b_R)$ for which $|p_0'(x_n, b_L, b_R)| < 1$. The balance between these two factors typically results in chaotic attractors. This controlled bifurcation to chaotic attractors is quite different from the appearance of spurious solutions due to discretization.

7. Conclusion

In this work we have applied modern computational tools to generalize the results of Kadyrov on the interaction of two hostile nations. We explored large regions of a four-dimensional parameter space and identified regions according to the number of critical points (equilibrium configurations of population groups in each of the two nations). We explored two basically different mathematical approaches (continuous versus discrete-time) to the modeling problem and showed that both methods agree in their predictions over a large range of parameters. The solutions of continuous models in two dimensions are restricted to critical points and limit cycles, but we identified parameter ranges for which the dynamics of the discrete model was more complex than that of the continuous model. For example, we found bifurcations to multiple periodic orbits and also to quasiperiodic attractors. We even found parameters for which the double-cusp system shows evidence for the existence of chaotic attractors. For the discrete model we were able to find all fixed-point solutions analytically, thereby avoiding numerical problems in difficult regions of the continuous model.

At this point we do not want to emphasize the applications of the Kadyrov model itself, but more the phenomenology and general analysis of the highly complex behavior arising in this simple model family. One main result of our exploration is the development of visualization tools to present the solutions embedded in a four-dimensional parameter space. Structures in the space of solutions and trends can be recognized directly in all four directions of variation of our model parameters. With the faster discrete model, this makes possible an almost interactive style of experimental mathematics, impossible with traditional approaches.

Several directions for future investigations of models of the Kadyrov type are suggested. The robustness of the model against stochastic perturbations (shocks) is currently under investigation using Chapman–Kolmogorov equations. Conditions under which chaos arises could be classified, especially in coupled systems of three or more cusps. We also hope to apply our models, in collaboration with political scientists, to concrete political questions.

Acknowledgements

It is a pleasure to acknowledge the generosity of Peter Brecke, James Keeler, Judy Challinger, Yoshi Oono, and Christopher Zeeman in sharing their ideas and resources. Timothy Poston has been most helpful in explaining the technicalities of topological and differentiable unfoldings, and we are grateful to him. The phase portraits of Fig. 2 were made with software

developed with the support of the U.S. Department of Energy's Applied Mathematical Sciences program at Brookhaven National Laboratory. Finally, we thank the University of California INCOR program, administered through the Center for Nonlinear Systems, Los Alamos National Laboratory, and its director, David Campbell, for the support which made this joint project possible. The numerical work was done in the Computational Mathematics Laboratory at the University of California at Santa Cruz, on a ring of Silicon Graphics Iris workstations, one loaned by Silicon Graphics Inc., through the good graces of Peter Broadwell, and one generously provided by Maria Schonbek.

References

Abraham, R. H. & Shaw, C. D. [1982–88] *Dynamics, The Geometry of Behavior*, Four vols. (Aerial Press, Santa Cruz, CA).

Abraham, R. H. [1986] "Mathematics and evolution: A manifesto," *IS Journal* **1**(3), 14–23.

Abraham, R. H. [1987] "Complex dynamics and the social sciences," *J. World Futures* **23**, 1–10.

Abraham, R. H. [1987] "Mathematics and evolution: A proposal," *Int. Synergy* **2**(2), 27–45.

Abraham, R. H. [1990] "Cuspoidal nets," in *Toward a Just Society for Future Generations*, ed. Banothy, B. A. & Banothy, B. H. (Int'l Society for the Systems Sciences) pp. 667–683.

Axelrod, B. [1984] *The Evolution of Cooperation* (Basic Books, New York).

Brams, S. [1985] *Superpower Games* (Yale University Press, New Haven, CT).

Callahan, J. [1982] "A geometric model of anorexia and its treatment," *Behavioral Science* **27**, 140–154.

Callahan, J. & Sashin, J. I. [1987] "Models of affect-response and anorexia nervosa," in *Perspectives in Biological Dynamics and Theoretical Medicine*, ed. Koslow, S. H., Mandell, A. J. & Shlesinger, M. F. (New York Academy of Sciences, New York).

Campbell, D. & Mayer-Kress, G. [1989] "Nonlinearity and chaos: The challenges and limitations of mathematical modeling of environmental and socio-political issues," in *Proc. Conf. on Technology-based Confidence Building: Energy and Environment, CNSS Papers No. 22.*

Forrest, S. & Mayer-Kress, G. [1989] "Using genetic algorithms in nonlinear dynamical systems and international security models," in *The Genetic Algorithms Handbook* (Van Nostrand Reinhold).

Grossmann, S. & Mayer-Kress, G. [1989] "The role of chaotic dynamics in arms race models," *Nature* **337**, 701–704.

Holsti, O. E. & Rosenau, J. N. [1988] "The domestic and foreign policy beliefs of American leaders," *J. Conflict Resolution* **32**(2), 248–294.

Isnard, C. A. & Zeeman, E. C. [1977] "Some models from catastrophe theory in the social sciences," in *Catastrophe Theory*, ed. Zeeman, E. C. (Addison-Wesley, New York) pp. 303–359.

Kadyrov, M. N. [1984] "A mathematical model of the relations between two states," *Global Development Processes* **3** (Institute for Systems Studies).

Kapral, R. [1985] "Pattern formation in two-dimensional arrays of coupled, discrete-time systems," *Phys. Rev.* **A31**, 3868.

Kapral, R. [1986] "Discrete models for the pattern formation and evolution of spatial structure in dissipative systems," *Phys. Rev.* **A33**, 4219–4231.

Keeler, J. [1987] *PhD Thesis* (University of California, San Diego, CA).

Mayer-Kress, G. [1991] "Nonlinear dynamical systems approach to international security," in *The Ubiquity of Chaos*, AAAS San Francisco, January 1989, ed. Krasner, S.

Oono, Y. & Puri, S. [1986] *Phys. Rev. Lett.* **58**, 836.

Oono, Y. & Yeung, C. [1987] "A cell dynamical system model of chemical turbulence," *J. Stat. Phys.* **48**, 593.

Poston, T. & Stewart, I. [1978] *Catastrophe Theory and its Applications* (Pitman, London).

Richardson, L. F. [1960a] *Arms and Insecurities; A Mathematical Study of the Causes and Origins of War* (Boxwood Press, Pittsburgh, PA).

Richardson, L. F. [1960b] *Statistics of Deadly Quarrels* (Boxwood Press, Pittsburgh, PA).

Smale, S. [1976] "A mathematical model of two cells via Turing's equation," in *The Hopf Bifurcation and its Applications*, ed. Marsden, J. E. and McCracken, M. (Springer, New York).

Wendroff, B. [1990] "On cooperation in a three-way arms race," Los Alamos preprint LA-UR-90-931.